EBioMedicine 2 (2015) 642–648

Contents lists available at ScienceDirect

EBioMedicine

journal homepage: www.ebiomedicine.com

Original Article

Bortezomib Amplifies Effect on Intracellular Proteasomes by Changing Proteasome Structure☆

David S. Pitcher, Kate de Mattos-Shipley, Konstantinos Tzortzis, Holger W. Auner, Anastasios Karadimitris, Maurits F. Kleijnen *

Centre for Haematology, Division of Experimental Medicine, Faculty of Medicine, Imperial College London, Hammersmith Campus, Commonwealth Building 4th Floor, Du Cane Road, London W12 0NN, United Kingdom

ARTICLE INFO

Article history:
Received 7 May 2015
Accepted 7 May 2015
Available online 28 May 2015

Keywords:
Multiple myeloma
Proteasome
Bortezomib
CTAB-PAGE
Posttranslational modification

ABSTRACT

The proteasome inhibitor Bortezomib is used to treat multiple myeloma (MM). Bortezomib inhibits protein degradation by inactivating proteasomes' active-sites. MM cells are exquisitely sensitive to Bortezomib – exhibiting a low-nanomolar IC^{50} – suggesting that *minimal* inhibition of degradation suffices to kill MM cells. Instead, we report, a low Bortezomib concentration, contrary to expectation, achieves severe inhibition of proteasome activity in MM cells: the degree of inhibition exceeds what one would expect from the small proportion of active-sites that Bortezomib inhibits. Our data indicate that Bortezomib achieves this severe inhibition by triggering secondary changes in proteasome structure that further inhibit proteasome activity. Comparing MM cells to other, Bortezomib-resistant, cancer cells shows that the degree of proteasome inhibition is the greatest in MM cells and only there leads to proteasome stress, providing an explanation for why Bortezomib is effective against MM but not other cancers.

© 2015 The Authors. Published by Elsevier B.V. This is an open access article under the CC BY license (http://creativecommons.org/licenses/by/4.0/).

1. Introduction

The proteasome inhibitor (PI) Bortezomib is used as a first- and second-line treatment of multiple myeloma (MM) (Anderson et al., 2011). Proteasomes' (Finley, 2009; Lander et al., 2012) main function is to degrade ubiquitinated proteins in a controlled manner (Bedford et al., 2011; Finley, 2009; Glickman and Ciechanover, 2002). Proteasomes are comprised of a cylindrical core particle (CP) capped at each end by a regulatory particle (RP) (Lander et al., 2012; He et al., 2012). The RP captures and denatures ubiquitin-marked protein substrates, and translocates their unfolded polypeptide chains towards proteolytic active-sites in the CP's lumen (Finley, 2009). CP contains three types of active-sites, each of which comprises a peptide-docking area and an exposed catalytic threonine. PIs including Bortezomib prevent protein hydrolysis by forming covalent adducts with the catalytic threonines of the active-sites (Groll et al., 2009; Beck et al., 2012). Some proteasome activity is necessary for any cell to live (Heinemeyer et al., 1997), not just MM cells (Craxton et al., 2012; Suraweera et al., 2012).

Although the Bortezomib concentrations at which cells of different cancers die differ widely, from low nanomolar to high micromolar IC^{50} concentrations, cells of the (incurable) B-cell malignancy MM are exquisitely sensitive (Shabaneh et al., 2013), hence Bortezomib's success in treatment of MM (Anderson et al., 2011). Intriguingly, Bortezomib at its low IC^{50} concentration causes only a small reduction in proteasomes' ability to degrade proteins (Kisselev et al., 2006; Shabaneh et al., 2013). The reduction is small because Bortezomib preferentially inhibits the chymotrypsin-like (CT-Like) active-site, but – at IC^{50} – does not inhibit the caspase-like and trypsin-like active-sites (Fig. S2A) (Kisselev et al., 2006); however, protein substrates can be hydrolysed by any of the three types of active-sites (Kessler et al., 2001; Kisselev et al., 2006). Thus, the question arises why minimal inhibition of proteasome function suffices to induce apoptosis in MM but not in Bortezomib-insensitive cells. Several explanations have been proposed, including high proteasome workload in MM cells (Bianchi et al., 2009; Meister et al., 2007; Shabaneh et al., 2013).

We report that, surprisingly, a (low) IC^{50} Bortezomib challenge – which in-vitro minimally inhibits proteasomes – in living MM cells severely inhibits proteasomes' hydrolytic activity. Our data suggest that, in living MM cells, a Bortezomib-induced structural change in the

☆ Research in context: Bortezomib and other proteasome inhibitors can treat multiple myeloma, a blood cancer arising from plasma B-cells, but few other cancers. It has been unclear why Bortezomib kills myeloma cells at concentrations so low that only partial inhibition of proteasomes is expected, and why Bortezomib cannot kill most other cancer cells. We now report that Bortezomib achieves unexpectedly severe inhibition of intracellular proteasomes, by triggering structural changes in these which further depress activity. Thus, Bortezomib 'punches above its weight' and achieves unexpectedly severe – sometimes lethal – levels of proteasome inhibition. The greatest inhibition happens exactly in cells from cancers which Bortezomib can treat.

* Corresponding author.
E-mail address: m.kleijnen@imperial.ac.uk (M.F. Kleijnen).

http://dx.doi.org/10.1016/j.ebiom.2015.05.016
2352-3964/© 2015 The Authors. Published by Elsevier B.V. This is an open access article under the CC BY license (http://creativecommons.org/licenses/by/4.0/).

proteasome (Pitcher et al., 2014) is responsible for this severe degree of proteasome inhibition.

2. Experimental procedures

Antibodies from Enzo Life Sciences: α-ubiquitin (FK2, PW8810), α-cleaved caspase 3 (PAb, ADI-AAS-103), α-20S α7 (MoAb LN43, BML-PW8110), α-Rpn12/S14 (PAb, BML-PW8815), α-Rpn10/S5a (MoAb S5a-18, BML-PW9250), α-Rpt5/S6a (MoAb TBP1-19, PW8770), α-Rpt4/S10b (MoAb p42-23, PW8830), α-Rpt2/S4 (PAb, BML-PW8305), and α-β5i/LMP7 (PAb, PW8355). Antibodies from other sources: α-streptag (Qiagen, MoAb 34850), α-PARP (CellSignalling, PAb, #9542) and α-procaspase3 (CellSignalling, PAb, #9661). CTAB-PAGE as described (Pitcher et al., 2014; Simpson, 2010). Additional Reagents: Ada-K(Biotin)-Ahx$_3$-L$_3$-VS, epoxomicin (Enzo LifeSciences), Bortezomib (Millennium/Takeda), Streptactin resin (Qiagen, 30004), Ni^{++}NTA resin (Sigma-Aldrich, His Select HF Nickel Affinity Gel, H0537 (Fig. 2c), or His Select agarose, P2266). AnnexinV/7AAD apoptosis staining (EBioscience 88-8007-74) was used to assess cell viability. Enzymes: DNase1, micrococcal nuclease, RNaseA/T1, RNaseH, S1 nuclease and RNAse1 (Fermentas/Thermo), PDE1 from *Crotalus adamanteus* venom (Sigma, P3243-1VL). Caspase Inhibitor Set III (Enzo Life Sciences, ALX-850-227-KI01), used at 1:500 dilution = 4 μM. Antibodies were diluted in PBS + 0.5% Tween20 for Western blotting, PVDF membranes were re-probed multiple times (Yeung and Stanley, 2009). Myeloma cell lines NCI-H929, KMS12-BM, RPMI-8226, OPM2, and the T-lymphocyte Jurkat cell line, were grown in RPMI (Sigma), supplemented with 10% v/v FBS, and 1% v/v Pen/strep. Cell fractionation procedure as described (Pitcher et al., 2014). For fractionation, a cytosol extraction (CE) buffer (25 mM Tris–HCl [pH 7.8], 5 mM $MgCl_2$/EDTA, 1 mM ATP/ADP, 2 mM DTT, 150 mM NaCl, 0.1 or 0.5% NP-40/IGEPAL) and nuclear extraction (NE) buffer (Bakondi et al., 2011) (20 mM HEPES [pH 7.4], 420 mM NaCl, 0.5 mM EDTA, 0.5 mM EGTA, 1 mM DTT, 1 tablet of inhibitor cocktail (Roche, 11-873-580-001) per 50 ml) were used. When using the NE for subsequent affinity-purification, 2 volumes of H_2O were added to 1 volume NE to reduce the NaCl concentration to physiological levels. For non-fractionated lysate, cell pellets snap-frozen in LN and stored at −80 °C were resuspended and combined in 10× volume of CE buffer and passed through a NanoDeBEE (BEE international) homogeniser at 19,000 PSI. Proteasome activity was measured basically as described (Kisselev and Goldberg, 2005; Vilchez et al., 2012), using fluorogenic proteasome substrates Suc-LLVY-AMC, Ac-RLR-AMC, Ac-GPLD-AMC (Enzo Life Sciences) for the three types of active-site. Cells were lysed in proteasome activity assay buffer (50 mM Tris–HCl, pH 7.5, 250 mM sucrose, 5 mM $MgCl_2$, 0.5 mM EDTA, 2 mM ATP and 1 mM DTT) by passing cells through a 29 G needle ten times. Fluorescence (380 nm excitation, 460 nm emission) was monitored continuously on a microplate fluorometer for 1 h at 37 °C. To measure for the presence of free 20S proteasomes, 0.015% SDS was added to the proteasome activity assay buffer (Fig. S2C). For each well, a second was set up with the addition of 40 mM Bortezomib; any activity in the Bortezomib wells was subtracted from corresponding wells to compensate for unspecific protease activity. The ubiquitinated substrate (G3P) (Matyskiela et al., 2013) was kindly provided by Dr Andreas Martin, and used as described. In-vitro degradation with purified yeast (Fig. S4) and human (Fig. 3C,D) proteasomes was done in PBS supplemented with 2.5 mM ATP, 2.5 mM $MgCl_2$, 2.5 mM DTT, and 10% DMSO in a total volume of 20 μl. Reaction was performed for 1 h either at 30 °C or 37 °C (Fig. 3C,D), after which the reaction was stopped by addition of 20 μl 2× SDS sample buffer and boiled.

Graphs were produced using Graph pad Prism 6. Data plotted were mean of replicates, with error bars plotted of the standard error of mean (SEM).

Research was supported by Leukaemia Lymphoma Research UK (LLR Grant10016 to MFK, LLR Gordon Piller Studentship award Grant11043 to MFK, AK, DP), by an MRC-Imperial Confidence-in-Concept (ICiC) grant to MFK, and by the NIHR Biomedical Research Centre at Imperial College NHS Trust, London.

3. Results

NCI-H929 MM cells were challenged with a lethal (10 nM) Bortezomib concentration for varying lengths of time. Cells were then lysed and an artificial fluorogenic peptide substrate was used to measure proteasomes' hydrolytic activity (Fig. 1a). Over 0–6/8 h, CT-like activity declined continually to almost nothing. Only when it was nearly absent (<10%), after 6–8 hour incubation, was an increase in ubiquitin conjugate levels observed; intracellular accumulation of ubiquitinated proteins indicates that proteolytic workload exceeds proteasome capacity, accumulation being a phenotype which integrates other regulatory mechanisms in the cell including deubiquitinating enzyme activity (Fig. 1a; see also Fig. S1A). However, when cells were first lysed and then challenged with 10 nM Bortezomib, only a 40% reduction in proteasomal (CT-like) activity was observed (Fig. S2A: 61.5% CT-like activity left, and as previously reported (Kisselev et al., 2006)). A much stronger-than-expected in-vivo inhibitory effect was also observed for the other types of proteasomal active-sites (Figs. S2E;S2C).

Predictable explanations for Bortezomib's severe inhibition of proteasomes' activity in MM cells did not apply: (1) severe inhibition was not due to prolonged incubation, because exposing *purified* proteasomes in the test tube to 10 nM Bortezomib for longer periods of time still showed modest inhibition in line with Fig. S2A (Figs. 1B; Fig. S1B) (Bianchi et al., 2009; Kisselev et al., 2006; Shabaneh et al., 2013). Furthermore, we identified a MM cell line, RPMI-8226, in which CT-like proteasome activity dropped very rapidly, within 2 h, to <10% (Fig. 1e); this time-frame approaches that of the in-vitro test using cell lysate (Fig. S2A), but in-vitro 61.5% of activity remains. (2) Although 10 nM Bortezomib induced apoptosis, and apoptosis is known to inhibit proteasomes via caspase activation (Sun et al., 2004; Adrain et al., 2004), caspase activation was not responsible for the observed proteasome inhibition: inhibition preceded caspase activation (Fig. 1c), occurred when caspase inhibitors were present (Fig. 1d), cells were alive until 10 h post-challenge as measured by Annexin-V staining (Fig. S2B), and there was a non-myeloma, T-lymphocyte cell line that did not die with 10 nM Bortezomib but in which proteasome activity still dropped well beyond expectation to ~20% (Figs. 1F,S2D; see also lung carcinoma A549 cells: Fig. S2D). (3) Severe inhibition was not because MM cells actively pumped in and/or retained Bortezomib to establish a 10–100 fold higher (Fig. S2A) intracellular Bortezomib concentration. We used the irreversible biotinylated inhibitor Ada-K(Biotin)-Ahx$_3$-L$_3$-VS (Kessler et al., 2001) to simultaneously measure inhibition of activity and the degree to which active-sites were inhibited, i.e. biotinylated (Kessler et al., 2001). We observed in-vivo a discrepancy between active-site inhibition and reduction in hydrolytic activity of those active-sites (Fig. 2a).

We now report a structural change in the proteasome which does correlate with Bortezomib-triggered early shutdown of proteasomal activity: Bortezomib-triggered early changes in posttranslational modifications on proteasomal subunits. We recently reported that human nuclear proteasomes carry a constitutive, CTAB-PAGE-detectable, post-translational modification that, in some respects, resembles poly(ADP)-ribose (Pitcher et al., 2014). We reported that exposing MM cells to Bortezomib induced changes in these CTAB-PAGE-detectable proteasome modifications, exactly at Bortezomib's IC^{50} concentration and above (Pitcher et al., 2014). Fig. 2b – CTAB-PAGE analysis of total cell lysate – shows that changes in these modifications of the proteasomal Rpn12 subunit occur between 1 h (RPMI-8226) and 4 h (H929) of PI challenge. To examine these Bortezomib-triggered changes in finer detail, we combined cell fractionation with affinity-purification of human proteasomes. (Purification is a technical trick that enables modified subunits to also become compatible with, and visible on, SDS-PAGE (Pitcher et al., 2014).) We generated retrovirally-transduced OPM2 MM cells, which expressed a Rpn11 subunit tagged N-terminally with

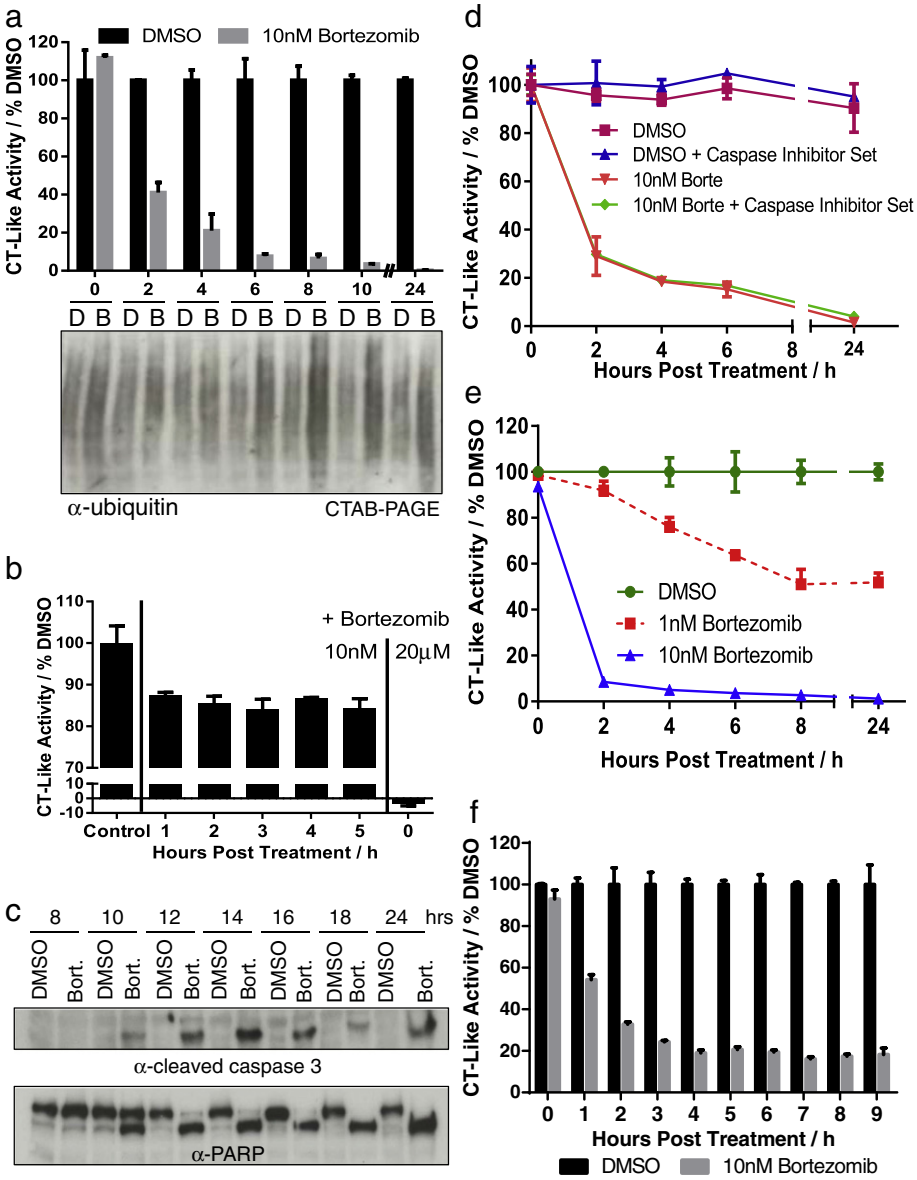

Fig. 1. Exposing myeloma cells to a lethal Bortezomib concentration leads to much greater inhibition of proteasomal hydrolytic activity in-vivo than is seen with cell lysate or purified proteasomes. (a) Measuring over time the effects on CT-like proteasome activity in Bortezomib-sensitive multiple myeloma cells (NCI-H929) after a 10 nM Bortezomib challenge (n = 2 per value). For the same time points, the degree of accumulation of ubiquitin conjugates in NCI-H929 cell lysate is visualised (see also Fig. S1A). Data represented as mean ± SEM. (b) Measuring the level of inhibition of purified human *26S* proteasomes following pre-incubation with 10 nM Bortezomib from 1 to 5 h at 4 °C (CT-Like activity was measured using Suc-LLVY-AMC at 37 °C). Data represented as mean ± SEM. Fig. S1B: experiment done also with yeast *26S* proteasomes, and with higher pre-incubation temperature. (c) Time course experiment with NCI-H929 cells, looking at caspase 3 activation and PARP cleavage (Substrate of Caspase 3), following a 10 nM Bortezomib challenge. (d) Investigating the effect of caspase inhibitors on Bortezomib's ability to shut down over time CT-Like activity in NCI-H929 cells. For experimental procedure, and validation that the procedure indeed inhibited caspases, see (Pitcher et al., 2014). Data represented as mean ± SEM (n = 2 per value). (e) Measuring over time the effects on CT-like proteasome activity in Bortezomib-sensitive multiple myeloma cells (RPMI-8226) after a DMSO, 1 nM (sub-lethal) and 10 nM (lethal) Bortezomib challenge. Data represented as mean ± SEM (n = 2 per value). (f) Measuring over time the effects on CT-like proteasome activity in the Bortezomib-insensitive T lymphocyte Jurkat cell line. Annexin-V staining showed that this 10 nM Bortezomib challenge did *not* induce cell death in the Jurkat cells. Data represented as mean ± SEM. See also Figs. S1,S2.

a His_6–StrepII–StrepII–TEV-affinity cassette. Cell fractionation and then affinity-purification (using streptactin or Ni^{++}NTA) showed that subunits from specifically nuclear proteasomes are extensively modified, as we reported previously (Pitcher et al., 2014) (Fig. 2c: Rpn11 subunit, detected with anti-streptag antibody). Repeating this fractionation-then-affinity-purification procedure, but this time after OPM2 cells had been treated with 20 nM (lethal) Bortezomib for up to 5–7 h, showed that patterns of modified subunits changed (Fig. 2d,e). These changes' characteristics depended on the particular proteasome subunit that was analysed. Generalising, these changes involved (A) a reduction in complexity for nuclear proteasomes (e.g. Rpt5, Rpn12), and/or (B) the appearance of modified subunit species in the cytosol fraction (e.g. β5i, Rpn12). (A) and (B) raise the possibility that severe inhibition of proteasome activity in total lysate (Fig. 1) may result from changes in proteasome structure which happen both in the cytosolic and nuclear compartments of the cell after cells are challenged with Bortezomib. We are currently investigating the exact nature of the proteasome modifications.

In order to test directly if changes in these proteasome modifications affect proteasome function, we first searched for commercial enzyme preparations that can digest the modifications of nuclear proteasomes. We discovered that a combination of venom phosphodiesterase-1 and S1 nuclease was efficient in trimming these modifications and collapsing modified Rpt2 species into its correct subunit-size species (Fig. 3A). Next,

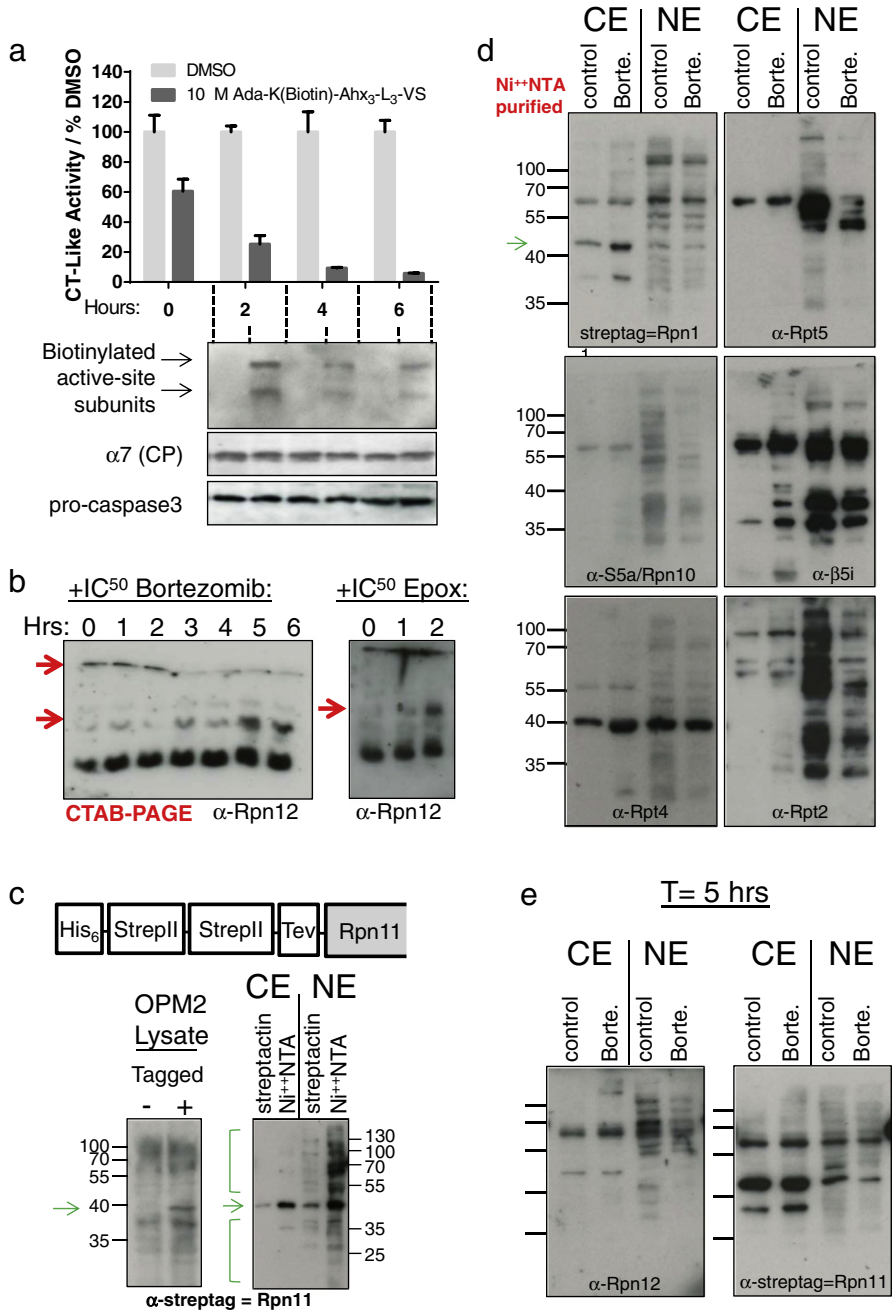

Fig. 2. Bortezomib's inhibition of proteasomal active-sites triggers changes in the structure of intracellular proteasomes. (a) Investigating the active-site occupation by proteasome inhibitor Ada-K(Biotin)-Ahx$_3$-L$_3$-VS, and proteasome activity remaining. NCI-H929 cells were incubated with 10 μM inhibitor for several hours, after which they were harvested and analysed for levels of inhibited/biotinylated active-sites, overall proteasome activity and pro-caspase-3 status (n = 2 per value). While the level of inhibited active-sites did not increase over time (and in fact was less in the 4- and 6-hour samples), we observed a steady decline in the activity of the CT-like active-sites in these samples. Ada-K(Biotin)-Ahx$_3$-L$_3$-VS-treated cells remained alive, as determined by Annexin-V/7AAD staining, for up to 10 h, and procaspase-3 levels stayed constant for the same time. Data represented as mean ± SEM. (b) NCI-H929 cells were incubated with 10 nM Bortezomib, RPMI-8226 cells with 20 nM epoxomicin, cells were lysed at specific time points and run on CTAB-PAGE (Pitcher et al., 2014). The resulting western was blotted for Rpn12. Note the changes in Rpn12 patterning over time upon lethal PI challenge. (c) OPM2 MM cells were retrovirally transduced to overexpress the Rpn11 proteasome subunit bearing an N-terminal affinity-tag (see schematic). Western blotting (left panel) of whole-cell lysate from transduced/non-transduced OPM2 cells using an α-streptag antibody shows expression of the tagged subunit (expected size Rpn11 + Tag = 35.6 kDa + 9 kDa = 44.6 kDa). Using this tagged MM cell line, the Western Blot panel on the right shows affinity-purification of proteasomes from both cytosolic (CE) and subsequent nuclear (NE) extract by Ni^{++}NTA or Streptactin capture. Extraction done as described (Pitcher et al., 2014), using 0.1% NP40 in CE buffer. Note that the many modified nuclear species of Rpn11 cannot be visualised on SDS-PAGE unless purified, and thus – after purification – appear on gel 'out of nowhere' (compare 'total lysate' panel on the left with purified 'CE/NE proteasome' panel on the right, green brackets), as reported previously (Pitcher et al., 2014). (d) Tagged proteasomes were affinity-captured with Ni^{++}NTA from CE and NE from 7-hour control- (PBS) or Bortezomib-treated (20 nM) Rpn11-tagged OPM2 cells. These proteasomes were run on SDS-PAGE, and then blotted for various proteasomal subunits. Extraction done as described (Pitcher et al., 2014), but CE buffer contained 0.5% NP40. (e) Same as in (d), but cells were harvested – and proteasomes were captured – after only 5 h of incubation with Bortezomib. See also Fig. S3.

we combined this enzyme protocol with an in-vitro proteasome-mediated proteolysis assay, which uses a ubiquitinated model protein as substrate (Matyskiela et al., 2013) (Figs. 3B, S4). We scaled up cell growth and affinity-purified proteasomes from total (i.e. including nuclear) lysate. Proteasomes bound to affinity-resin were mock-treated or treated with PDE1/S1 at a sub-optimal (20 °C) temperature, after which resin was washed to remove enzymes. Next, proteasomes were eluted to generate a control and a PDE1/S1-treated proteasome

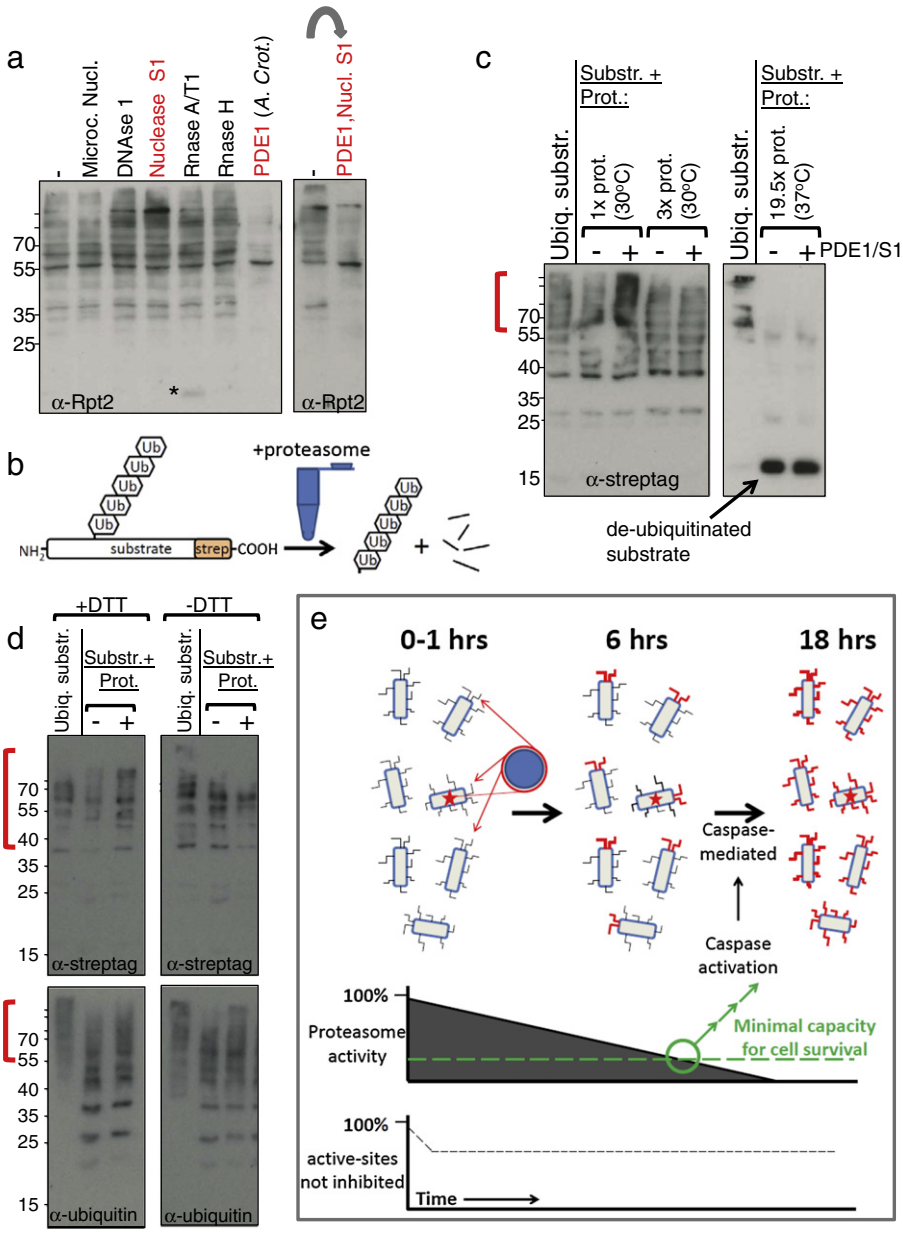

Fig. 3. Manipulating proteasome modifications changes proteasome function. (a) Affinity-purified nuclear proteasomes were incubated with the indicated enzymes for 1 h at 37 °C, subjected to SDS-PAGE, and analysed by Western Blot for proteasome subunit Rpt2. (b) Schematic presentation of the in-vitro proteasome-mediated proteolysis assay, which uses a ubiquitinated model protein as substrate (Matyskiela et al., 2013). In this system, proteasomes degrade the protein substrate while releasing the multiubiquitin chains in intact form (Fig. S4D). (c) Human proteasomes from Rpn11-tagged OPM2 cells were affinity-purified by Ni^{++}-NTA agarose capture of the His_6 domain. Half the prep was incubated on the beads in reaction buffer, while the other with reaction buffer and PDE1 + S1 combination, for 50 min at 20 °C before being eluted in 250 mM Imidizole-PBS. Varying relative amounts of proteasomes/substrate 1×, 3× were added to G3P model substrate and incubated for 1 h at 30 °C (in the presence of ATP, $MgCl_2$ and DTT) before running on SDS-PAGE and blotted against the Strep domain on the model substrate. Panel on the right: incubated at 37 °C and 19.5× proteasomes to substrate. (d) As in (c), but comparing enzyme-treated and control-treated proteasomes for ability to degrade ubiquitinated protein substrate in reducing (+DTT) and oxidizing reaction conditions. Analysis is done using streptag (substrate) and ubiquitin antibodies. (e) We propose the following model of how PIs virtually shut down proteolysis in cells while inhibiting few active-sites throughout. 2 h after exposing myeloma cells to an IC^{50} Bortezomib challenge (5–10 nM), only a small proportion of active-sites have been inhibited (red star). This proportion does not increase and, as a result, proteolysis is, in this initial period, almost unaffected due to uninhibited active-sites. However, over the next several hours, proteasomes' CTAB-PAGE-detectable modifications change (red), causing proteasome activity to decline. When proteolysis falls below the level required for life, caspases are activated and cells go through programmed cell death. See also Fig. S4.

preparation. Most subunits of PDE1/S1-treated versus untreated proteasomes were very similar, but for example Rpn12 showed pronounced differences (Fig. S3). We then incubated the proteasome preparations with a ubiquitinated model protein (Matyskiela et al., 2013) (Fig. S4) in order to assess the ability of these proteasome preparations to process a ubiquitinated substrate. At low proteasome/substrate ratio at 30 °C, the PDE1/S1-treated proteasomes were impaired in degrading ubiquitinated substrate (Fig. 3C). However, increasing the ratio overcame this defect, with both preparations degrading substrate equivalently. At even higher proteasome/substrate ratio, and at 37 °C, proteasomes processed the substrate towards deubiquitination rather than degradation, and again both preparations behaved equivalently (Fig. 3B). In addition, we found that changes in the redox state of the reaction conditions uncovered qualitative differences between enzyme-treated and untreated proteasomes (Fig. 3D): in the oxidizing conditions minus DTT, enzyme-treated proteasomes removed streptag epitope (i.e. substrate) more efficiently than untreated proteasomes but did not shift down the ubiquitin signal correspondingly, indicating that these enzyme-treated

proteasomes only partially digested the substrate protein – starting from the tagged carboxyterminus – before premature release. In contrast, under reducing conditions, untreated proteasomes were more efficient in degrading substrate than enzyme-treated proteasomes (see also Fig. 3C). In sum, our data indicate that, under certain experimental conditions, changes in proteasome modifications affect proteasome function, thereby strengthening the case that Bortezomib-triggered changes in proteasome modifications within cells also affect proteasome function.

4. Discussion

In summary, our data reveal a dramatic inhibition of proteasome activity in MM cells after a (low) IC^{50} Bortezomib challenge, and suggest that this inhibition is the *compound* result of, first, inhibition of a subset of active-sites, and, second, structural changes in the proteasome which further impair hydrolytic activity (Fig. 3E). Engagement of PIs with active-sites changes proteasome conformation and stabilizes the (distant) CP–RP (Kleijnen et al., 2007; Park et al., 2008) and RP-hPLIC/ubiquilin (Kleijnen et al., 2000) interactions, thus providing a possible signalling mechanism into the cell that may enable active-site inhibition to directly trigger activation of the cellular machinery that then changes the posttranslational modifications of the proteasomes. Whereas it has been very difficult to explain why MM cells die from a nanomolar IC^{50} Bortezomib challenge when assuming that the modest level of proteasome inhibition observed in-vitro holds true in-vivo (Bianchi et al., 2009; Kisselev et al., 2006; Shabaneh et al., 2013), it is not surprising that a myeloma cell with over 95% CT-inhibition and observable proteasome stress (i.e. accumulation of ubiquitin conjugates, Fig. 1a) will undergo apoptosis. In addition, our data show that Bortezomib, in cancer cells which are Bortezomib-resistant, does not achieve the same degree of proteasome inhibition as in (Bortezomib-sensitive) MM cells (Figs. 1F, S2D), thus providing a molecular mechanism explaining what differentiates MM from most other cancers which Bortezomib cannot treat. Please note that our data indicate that a high proteasome workload in MM cells (Bianchi et al., 2009; Meister et al., 2007; Shabaneh et al., 2013) cannot be the primary reason for MM cells' sensitivity to Bortezomib: for this explanation to work, all proteasomes in a cell would need to be fully engaged – with no spare capacity left – in order for a minimal inhibition of proteasomes to produce proteasome stress; instead, we observed that MM cells have much spare proteasome capacity, and that reducing capacity even to 20% still did not yield proteasome stress (Fig. 1a). Understanding the cellular mechanism via which Bortezomib amplifies its effect on proteasome function may enable future intervention to re-sensitize Bortezomib-resistant cells to treatment.

Authorship contributions

DSP designed, performed research, analysed data, and wrote manuscript. KdM-S, KT designed, performed research and analysed data. HWA, AK designed research and analysed data. MFK designed, performed research, analysed data, and wrote manuscript.

Disclosure of conflicts of interest

The authors declare that they have no conflict of interest.

Acknowledgements

The authors would like to thank Prof. Irene Roberts for helpful discussions.

Appendix A. Supplementary data

Supplementary data to this article can be found online at http://dx.doi.org/10.1016/j.ebiom.2015.05.006.

References

Adrain, C., Creagh, E.M., Cullen, S.P., Martin, S.J., 2004. Caspase-dependent inactivation of proteasome function during programmed cell death in Drosophila and man. J. Biol. Chem. 279, 36923–36930.

Anderson, K.C., Richardson, P.G., Ghobrial, I.M., 2011. Bortezomib in the Treatment of Multiple Myeloma. Springer, Basel.

Bakondi, E., Catalgol, B., Bak, I., Jung, T., Bozaykut, P., Bayramicli, M., Ozer, N.K., Grune, T., 2011. Age-related loss of stress-induced nuclear proteasome activation is due to low PARP-1 activity. Free Radic. Biol. Med. 50, 86–92.

Beck, P., Dubiella, C., Groll, M., 2012. Covalent and non-covalent reversible proteasome inhibition. Biol. Chem. 393, 1101–1120.

Bedford, L., Lowe, J., Dick, L.R., Mayer, R.J., Brownell, J.E., 2011. Ubiquitin-like protein conjugation and the ubiquitin–proteasome system as drug targets. Nat. Rev. Drug Discov. 10, 29–46.

Bianchi, G., Oliva, L., Cascio, P., Pengo, N., Fontana, F., Cerruti, F., Orsi, A., Pasqualetto, E., Mezghrani, A., Calbi, V., Palladini, G., Giuliani, N., Anderson, K.C., Sitia, R., Cenci, S., 2009. The proteasome load versus capacity balance determines apoptotic sensitivity of multiple myeloma cells to proteasome inhibition. Blood 113, 3040–3049.

Craxton, A., Butterworth, M., Harper, N., Fairall, L., Schwabe, J., Ciechanover, A., Cohen, G.M., 2012. NOXA, a sensor of proteasome integrity, is degraded by 26S proteasomes by an ubiquitin-independent pathway that is blocked by MCL-1. Cell Death Differ. 19, 1424–1434.

Finley, D., 2009. Recognition and processing of ubiquitin–protein conjugates by the proteasome. Annu. Rev. Biochem. 78, 477–513.

Glickman, M.H., Ciechanover, A., 2002. The ubiquitin–proteasome proteolytic pathway: destruction for the sake of construction. Physiol. Rev. 82, 373–428.

Groll, M., Huber, R., Moroder, L., 2009. The persisting challenge of selective and specific proteasome inhibition. J. Pept. Sci. 15, 58–66.

He, J., Kulkarni, K., Da Fonseca, P.C.A., Krutauz, D., Glickman, M.H., Barford, D., Morris, E.P., 2012. The structure of the 26S proteasome subunit Rpn2 reveals its pc repeat domain as a closed toroid of two concentric alpha-helical rings. Structure 20, 513–521.

Heinemeyer, W., Fischer, M., Krimmer, T., Stachon, U., Wolf, D.H., 1997. The active sites of the eukaryotic 20 S proteasome and their involvement in subunit precursor processing. J. Biol. Chem. 272, 25200–25209.

Kessler, B.M., Tortorella, D., Altun, M., Kisselev, A.F., Fiebiger, E., Hekking, B.G., Ploegh, H.L., Overkleeft, H.S., 2001. Extended peptide-based inhibitors efficiently target the proteasome and reveal overlapping specificities of the catalytic beta-subunits. Chem. Biol. 8, 913–929.

Kisselev, A.F., Goldberg, A.L., 2005. Monitoring activity and inhibition of 26S proteasomes with fluorogenic peptide substrates. Methods Enzymol. 398, 364–378.

Kisselev, A.F., Callard, A., Goldberg, A.L., 2006. Importance of the different proteolytic sites of the proteasome and the efficacy of inhibitors varies with the protein substrate. J. Biol. Chem. 281, 8582–8590.

Kleijnen, M.F., Shih, A.H., Zhou, P., Kumar, S., Soccio, R.E., Kedersha, N.L., Gill, G., Howley, P.M., 2000. The hPLIC proteins may provide a link between the ubiquitination machinery and the proteasome. Mol. Cell 6, 409–419.

Kleijnen, M.F., Roelofs, J., Park, S., Hathaway, N.A., Glickman, M., King, R.W., Finley, D., 2007. Stability of the proteasome can be regulated allosterically through engagement of its proteolytic active sites. Nat. Struct. Mol. Biol. 14, 1180–1188.

Lander, G.C., Estrin, E., Matyskiela, M.E., Bashore, C., Nogales, E., Martin, A., 2012. Complete subunit architecture of the proteasome regulatory particle. Nature 482, 186–191.

Matyskiela, M.E., Lander, G.C., Martin, A., 2013. Conformational switching of the 26S proteasome enables substrate degradation. Nat. Struct. Mol. Biol. 20, 781–788.

Meister, S., Schubert, U., Neubert, K., Herrmann, K., Burger, R., Gramatzki, M., Hahn, S., Schreiber, S., Wilhelm, S., Herrmann, M., Jack, H.-M., Voll, R.E., 2007. Extensive immunoglobulin production sensitizes myeloma cells for proteasome inhibition. Cancer Res. 67, 1783–1792.

Park, E., Lee, J.W., Eom, S.H., Seol, J.H., Chung, C.H., Nov 28 2008. Binding of MG132 or deletion of the Thr active sites in HslV subunits Increases the affinity of HslV protease for HslU ATPase and makes this interaction nucleotide-independent. J. Biol. Chem. 283 (48), 33258–33266. http://dx.doi.org/10.1074/jbc.M805411200 (Epub 2008 Oct 6).

Pitcher, D.S., De Mattos-Shipley, K., Wang, Z., Tzortzis, K., Goudevenou, K., Flynn, H., Bohn, G., Rahemtulla, A., Roberts, I., Snijders, A.P., Karadimitris, A., Kleijnen, M.F., 2014. Nuclear proteasomes carry a constitutive posttranslational modification which derails SDS-PAGE (but not CTAB-PAGE). Biochim. Biophys. Acta 1844, 2222–2228.

Shabaneh, T., Downey, S., Goddard, A., Screen, M., Lucas, M., Eastman, A., Kisselev, A., 2013. Molecular basis of differential sensitivity of myeloma cells to clinically relevant bolus treatment with Bortezomib. PLoS One 8.

Simpson, R.J., Apr 2010. CTAB-PAGE. Cold Spring Harb. Protoc. 2010 (4), 460–462. http://dx.doi.org/10.1101/pdb.prot5412 (pdb.prot5412).

Sun, X.-M., Butterworth, M., Macfarlane, M., Dubiel, W., Ciechanover, A., Cohen, G.M., 2004. Caspase activation inhibits proteasome function during apoptosis. Mol. Cell 14, 81–93.

Suraweera, A., Munch, C., Hanssum, A., Bertolotti, A., 2012. Failure of amino acid homeostasis causes cell death following proteasome inhibition. Mol. Cell 48, 242–253.

Vilchez, D., Boyer, L., Morantte, I., Lutz, M., Merkwirth, C., Joyce, D., Spencer, B., Page, L., Masliah, E., Berggren, W.T., Gage, F.H., Dillin, A., 2012. Increased proteasome activity in human embryonic stem cells is regulated by PSMD11. Nature 489, 304–308.

Yeung, Y.-G., Stanley, E.R., 2009. A solution for stripping antibodies from polyvinylidene fluoride immunoblots for multiple reprobing. Anal. Biochem. 389, 89–91.